IOP Conference Series: Materials Science and Engineering

PAPER • **OPEN ACCESS**

Transient simulation of melt flow, clogging, and clog fragmentation inside SEN during steel continuous casting

To cite this article: H Barati *et al* 2023 *IOP Conf. Ser.: Mater. Sci. Eng.* **1281** 012025

Transient simulation of melt flow, clogging, and clog fragmentation inside SEN during steel continuous casting

H Barati[1,2*], M Wu[2*], A Kharicha[2,3], A Ludiwg[2]

[1] K1-MET, Franz-Josef Street 18, 8700 Leoben, Austria
[2] Chair for Modeling and Simulation of Metall. Processes, Dept. Metall., Montanuniversitaet Leoben, Franz-Josef Street 18, 8700 Leoben, Austria
[3] Christian-Doppler Laboratory for Metallurgical Applications of Magnetohydrodynamics, Dept. Metall., Montanuniversitaet Leoben, Franz-Josef Street 18, 8700 Leoben, Austria

E-mail: hadi.barati@k1-met.com, menghuai.wu@unleoben.ac.at

Abstract. Clogging of submerged entry nozzle (SEN) during continuous casting of steel is an undesirable phenomenon leading to different problems like flow blockage, slag entrainment, nonuniform solidification, etc. A transient numerical model for nozzle clogging based on an Eulerian-Lagrangian approach was developed and it covers the main steps of clogging: (a) formation of the first oxide layer by chemical reactions on the steel-refractory interface; (b) motion of non-metallic inclusions (NMIs) due to the turbulent melt flow towards the SEN wall; (c) interactions between the melt, the NMI, and the wall; (d) formation and growth of the clog by the deposition of NMIs on the clog front and the flow-clog interactions; and (e) detachment/fragmentation of a part of clog due to the flow drag force. Clogging in an industrial scale SEN was simulated. The simulated clog front was compared with real as-clogged SENs. The modeling results have successfully explained the SEN clogging induced transient flow phenomenon in the mold region, i.e. the transition from the stable to an unstable and non-symmetrical flow.

1. Introduction

Clogging of submerged entry nozzle (SEN) during continuous casting (CC) of steel appears due to the build-up of solid materials on the inner wall. SEN clogging may lead to decreased productivity of the CC process and lower quality of the final product. Various clogging mechanisms have been proposed: attachment of non-metallic inclusions (NMIs) [1–3], reaction at the SEN wall [4–6], and temperature drop leading to solidification of steel or precipitation of alumina [7–9]. Among them, the deposition of NMIs on the SEN wall is still the primary cause of clogging [10].

Clogging has been studied experimentally and numerically for decades. In experimental studies, the main focus was on the analysis of clog [6,11], non-metallic inclusions [12,13], and effect of the steel composition [14,15]. The characteristics of these materials were correlated to clogging phenomena. Clogging can be generally considered in five steps, as depicted in Figure 1: (a) formation of the first oxide layer by chemical reactions on the steel-refractory interface; (b) transport of non-metallic inclusions (NMIs) by turbulent fluid flow towards the wall; (c) interactions between the fluid and the wall, and adhesion of the NMI on the wall; (d) formation and growth of the clog by the NMI deposition on the clog front and the flow-clog interactions; (e) detachment/fragmentation of a part of clog due to the flow drag force.

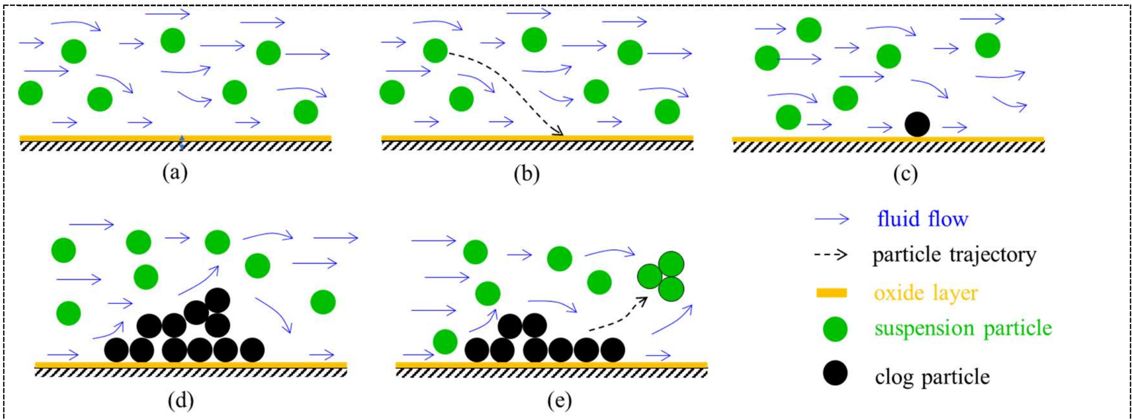

Figure 1. Schematic of main steps of clogging. (a) formation of the first oxide layer by chemical reactions; (b) transport of NMIs; (c) adhesion of the NMI on the SEN wall; (d) growth of the clog; and (e) detachment/fragmentation.

Different numerical models have been developed by considering one or more main steps of clogging. Single-phase-based Eulerian approach [10,16], Eulerian-Lagrangian approach [17–20], Eulerian-Eulerian two-phase approach [21,22] were tried to simulate clogging phenomena. Computational thermodynamics has also been adopted to investigate reactions and inclusion formation which are responsible for clogging [1,23,24]. Recently water models have also been considered to study the effects of as-clog SEN on the flow pattern inside the mold region [25].

The current authors have developed a transient model for nozzle clogging in steel CC that covers chemical reactions on the SEN refractory called 'early stage' of clogging [26] , i.e. step (a), along with clog growth due to NMI deposition called 'late stage' of clogging [27,28], i.e. steps (b) – (d) in Figure 1. The model was validated with laboratory experiments [27] and its accuracy and efficiency were verified for industry SENs [29]. In this work, the model is extended to consider one more sub-model for the detachment/fragmentation of a part of clog due to the flow drag force, i.e. step (e) in Figure 1.

2. Modeling

Eulerian–Lagrangian and volume-averaged approaches were adopted to simulate melt flow, NMI tracking, clogging, and fragmentation in a coupled way. The Eulerian approach was employed to calculate the turbulent flow and the Lagrangian approach was used to track the motion of the NMIs. A volume-average scheme is used to define the clog as a porous medium and track the growth of the clog. Details of this model were explained previously [27].

Modeling concept of clog fragmentation is schematically described in Figure 2. In the clogging model, clog is supposed to be a porous medium formed by random deposition of solid NMIs due to the turbulent flow, like Figure 2(a). This assumption is compatible with NMI networks observed in metallographic images of clog [16,30]. It is further assumed that the flow-induced drag force leads to mechanical fracture of the clog network, hence fragmentation of a part of the clog. To calculate the stress on the clog, the clog network is treated as a bunch of cylinders uniformly distributed, as shown in Figure 2 (b). Each cylinder called 'clog finger' is made out of sintered spheres, as shown in Figure 2 (c). The maximum stress occurs at the base of a clog finger. A similar idea was used by Pilling and Hellawell [31] to model the fragmentation mechanism for dendritic arms during solidification. They considered the dendrite as a cylinder with different radii between the root and main section. Similarly, clog finger was assumed to be a cylinder but with different radius at the base and flow is perpendicular to the clog finger, as shown in Figure 2(c). At the base of the clog finger, neck radius (r_n), increases over time due to the sintering. According to the calculations of Pilling and Hellawell, the maximum stress on the base of a clog finger (σ_n) is

$$\sigma_\mathrm{n} = \frac{2FL_\mathrm{c}^2}{\pi r_\mathrm{n}^3}, \tag{1}$$

where F is the total force acting on the clog finger by the melt flow. L_c and r_n are length of clog finger and neck radius due to sintering at the base of clog finger, respectively, as shown in Figure 2. Neck radius can be calculated by the theory of the kinetic growth of sintering neck of spheres,

$$\frac{r_\mathrm{n}^m}{r_\mathrm{p}^n} = A_{(T)}\, t \tag{2}$$

where r_p is radius of sphere and $A_{(T)}$ is a temperature-dependent constant expressed as

$$A_{(T)} = \frac{K_1 \gamma V_0 D}{RT} \tag{3}$$

In this equation, K_1 is a constant; γ is the interfacial tension; V_0 is the molar volume; D is the self-diffusion coefficient of the material; R is the gas constant; and T is the temperature. The exponents m and n in Equation (2) define the sintering mechanism. Here, $m = 5$ and $n = 2$ according to the experimental observation of sintering alumina spheres in steel melt [32].

If the calculated σ_n is larger than the strength of alumina, the clogged part in the computational cell is removed and a partially-clogged cell turns into a free cell. The strength of alumina was considered as 300 MPa, as reported in the literature [9,33,34].

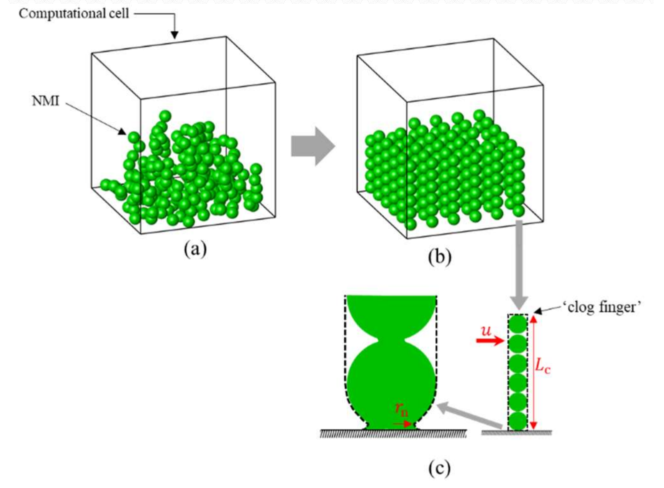

Figure 2. Schematic of fragmentation concept. (a) clog network constructed by random deposition of NMIs, (b) simplification of the clog network as a bunch of uniformly-distributed 'clog finger', (c) graphical description of the 'clog finger' as cylinder.

To test the model, a computational domain with boundaries is shown in Figure 3. The main objective of this work is to simulate melt flow and clogging inside SEN; however, a part of the CC mold was also included to have a reasonable flow pattern near the ports of SEN. In this case, accurate flow in the mold and cooling regions was not of interest. Hence, only a small length of mold and cooling part was included in the domain. At inlet, the mass flow rate of steel melt was 53.82 kg/s. Spherical alumina particles were injected with zero velocity and a rate of 0.0034 kg/s corresponding to 30 ppm oxygen content of the steel melt in the tundish before entering SEN. The particle size was 10 µm. Non-slip flow boundary conditions were considered for walls of SEN and CC mold and a shear-free wall was set for the free surface. The pressure outlet was set at the outlet. A clean SEN without any clogging is set as initial condition.

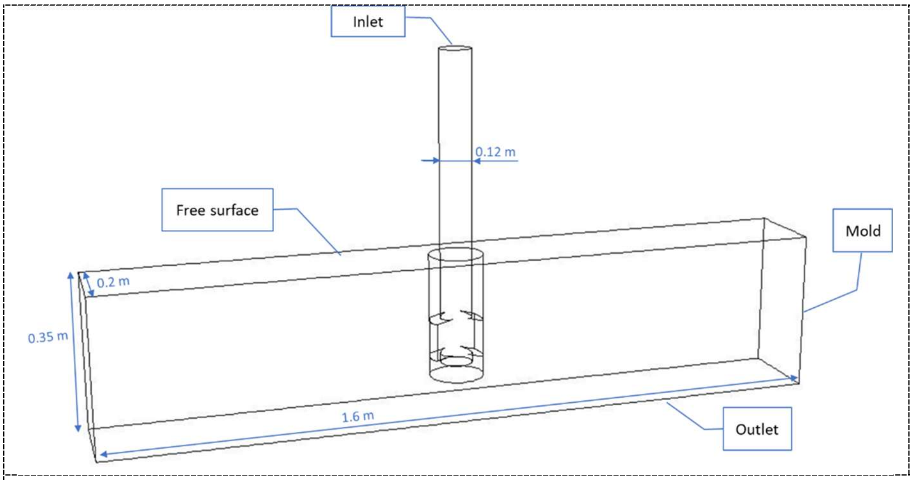

Figure 3. Computational domain and boundary conditions.

3. Results and discussions

In Figure 4, the transient growth of clog inside the SEN is plotted. For better visualization, the SEN is cut into two halves. It shows that clogging occurred initially at the bottom and ports. Then clogging continued on the tube part of the SEN. The random deposition of NMIs due to the turbulent melt flow resulted in random growth of the clog. The total clog fragmentation volume in each computational cell is shown in form of spheres in Figure 5. Because of continuous deposition and fragmentation, the total fragmentation volume in each cell could be larger than the cell volume. The major fragmentation occurred in the port area. Fragmentation in the bottom part was very small compared to that of the port area. With the evolution of clogging the major fragmentation area changed: in 9 min and 15 min, fragmentation was dominant on the side and bottom of the port area, but in 21 min and 27 min, the main fragmentation area was only the bottom of the ports. Fragmentation in the tube part was nearly uniform during the time. Another point is that the fragmentation in two halves of SEN was noticeably different after 9 min.

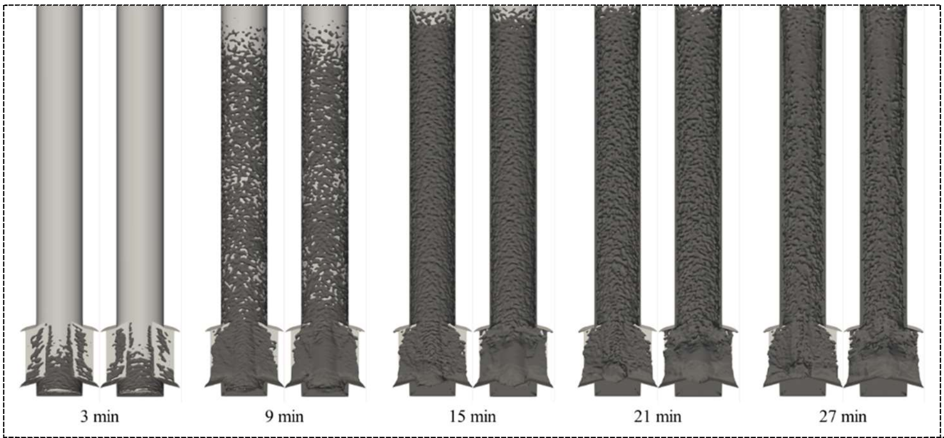

Figure 4. Growth of clog during the time.

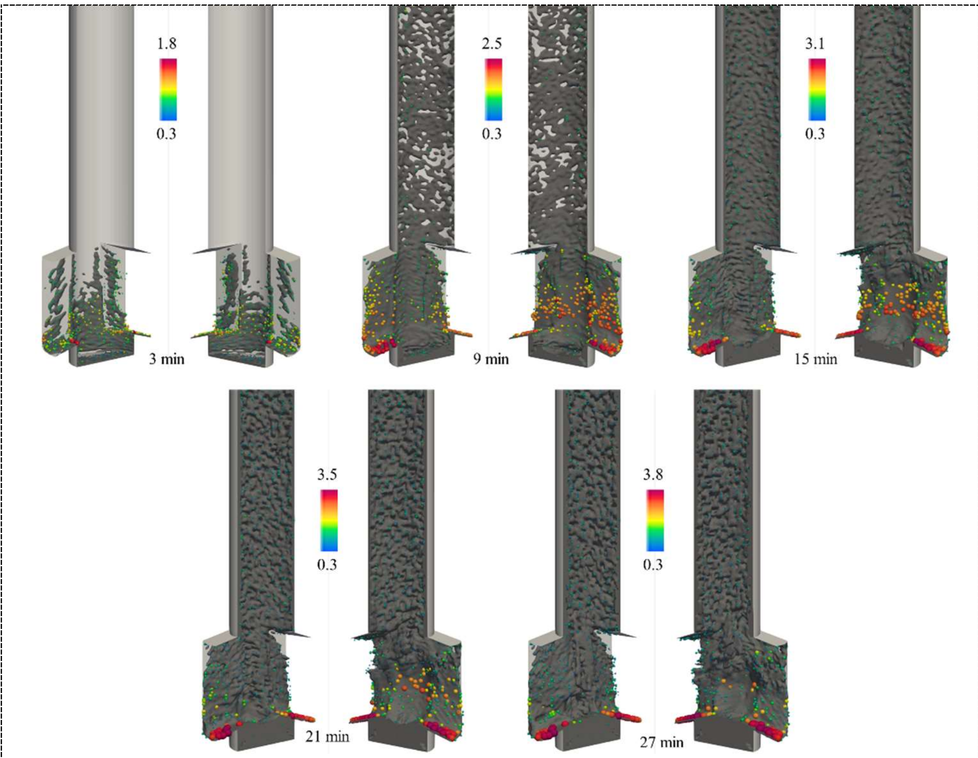

Figure 5. Clog front (grey) and total fragmentation volume (in form of colored spheres) during the time. Color bars show radius of spheres in mm.

In Figure 6, the flow inside the SEN is depicted. This figure shows that before 9 min, the flow in the ports was still conventional straight jets similar to that of non-clogged SEN. However, after 9 min, clog growth changed the flow, and a big vortex formed in the port area which lasted until the end of the simulation. This vortex explains why clog growth in the two halves of the SEN was very different.

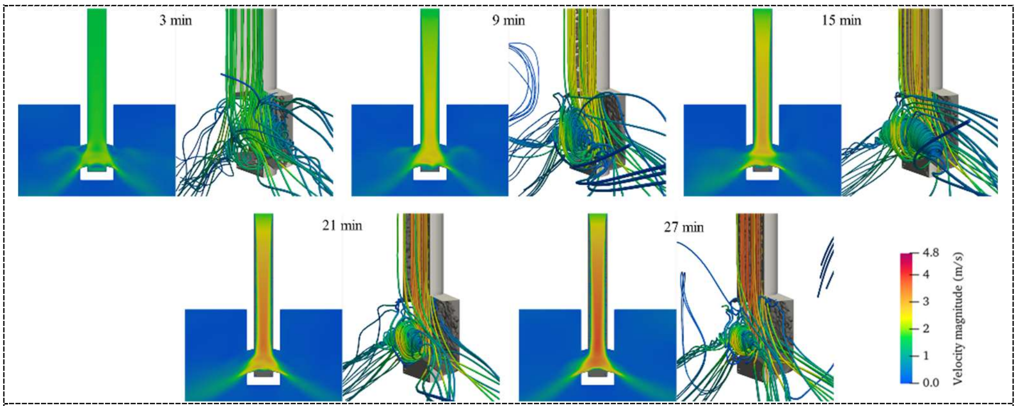

Figure 6. Melt flow on a symmetrical plane and flow streamlines inside the SEN during the time.

A qualitative comparison of as-clogged SENs from literature with the current simulation results, as shown in Figure 7, indicated that the current model has the potential to reproduce the clogging in real-size SENs. However, the proposed fragmentation sub-model requires still further refinements and improvements, like the treatment of turbulence in partially-clogged cells and the implementation of size and shape of NMIs.

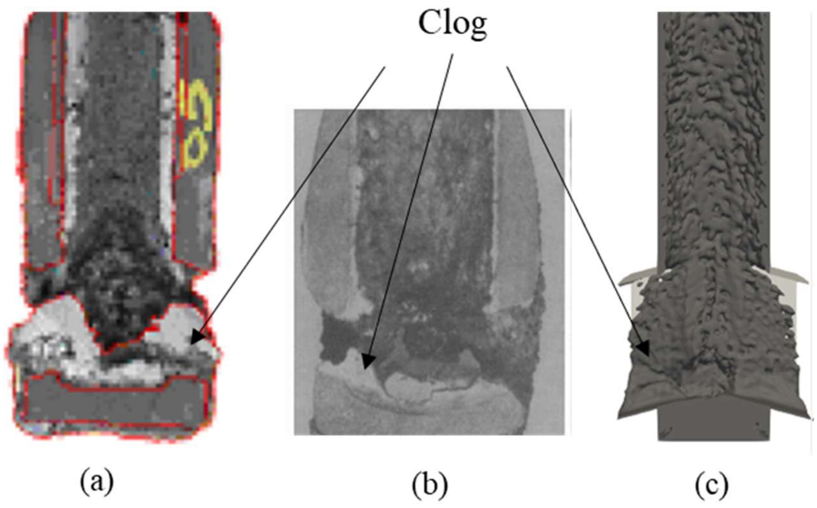

Figure 7. Qualitative comparison of as-clogged SENs, (a) from reference [8] and (b) from reference [16] with (c) the current simulation results.

4. Conclusions

A sub-model was developed for fragmentation during clogging in the continuous casting of steel. The sub-model was implemented in a transient clogging model. The simulation results of an industrial real-size SEN showed that after a while (in this case-study 9 min), the melt flow inside the SEN changed dramatically. This led to non-symmetrical growth of the clog, especially in the port area, and consequently non-symmetrical flow in the mold region. The addition of this feature to the developed clogging model made the model more realistic and more practical to study clogging in steel continuous casting.

Acknowledgements

The authors gratefully acknowledge the funding support of K1-MET GmbH, metallurgical competence center. The research program of the K1-MET competence center is supported by COMET (Competence Center for Excellent Technologies), the Austrian program for competence centers. COMET is funded by the Federal Ministry for Climate Action, Environment, Energy, Mobility, Innovation, and Technology; the Federal Ministry for Digital and Economic Affairs; the Federal States of Upper Austria, Tyrol, and Styria; and the Styrian Business Promotion Agency (SFG). In addition to the public funding from COMET, this research project was partially financed by scientific partners (Montanuniversität Leoben and Johannes Kepler University Linz) and industrial partners (voestalpine Stahl Linz GmbH, voestalpine Stahl Donawitz GmbH, and RHI Magnesita GmbH).

References

[1] Lee J-H, Kang M-H, Kim S-K and Kang Y-B 2018 Oxidation of Ti Added ULC Steel by CO Gas Simulating Interfacial Reaction between the Steel and SEN during Continuous Casting *ISIJ International* **58** 1257–66

[2] Vermeulen Y, Coletti B, Blanpain B, Wollants P and Vleugels J 2002 Material evaluation to prevent nozzle clogging during continuous casting of Al killed steels *ISIJ International* **42** 1234–40

[3] Sasai K and Mizukami Y 1994 Reaction Mechanism between Alumina Graphite Immersion Nozzle and Low Carbon Steel. *ISIJ International* **34** 802–9
[4] Miki Y, Kitaoka H, Sakuraya T and Fujii T 1992 Mechanism for separating inclusions from molten steel stirred with a rotating magnetic field *ISIJ International* **Vol. 32** 142–9
[5] Zhang L and Thomas B G 2006 State of the art in the control of inclusions during steel ingot casting *Metallurgical and Materials Transactions B* **37** 733–61
[6] Basu S, Choudhary S K and Girase N U 2004 Nozzle Clogging Behaviour of Ti-bearing Al-killed Ultra Low Carbon Steel *ISIJ International* **44** 1653–60
[7] Duderstadt G C, Iyengar R K and Matesa J M 1968 Tundish nozzle blockage in continuous casting *JOM* **20** 89–94
[8] Rödl S, Schuster H, Ekerot S, Xia G, Veneri N, Ferro F, Baragiola S, Rossi P, Fera S, Colla V and others 2012 *New strategies for clogging prevention for improved productivity and steel quality*
[9] Rackers K G and Thomas B G 1995 Clogging in Continuous Casting Nozzles *78th Steelmaking Conference Proceedings* vol 78 pp 723–34
[10] Bai H and Thomas B G 2001 Turbulent flow of liquid steel and argon bubbles in slide-gate tundish nozzles: Part I. model development and validation *Metallurgical and Materials Transactions B* **32** 253–67
[11] Karnasiewicz B and Zinngrebe E 2019 Observational Study of Clogging Specimens from the Tundish Well Showing Origin and Growth of a Clog in an Al-Killed Ti-Alloyed Steel Cast *Metallurgical and Materials Transactions B* **50** 1704–17
[12] Michelic S K and Bernhard C 2022 Significance of Nonmetallic Inclusions for the Clogging Phenomenon in Continuous Casting of Steel—A Review *Steel Res Int* **93** 2200086
[13] Zhang L F and Thomas B G 2003 State of the Art in Evaluation and Control of Steel Cleanliness *ISIJ International* **43** 271–91
[14] Dorrer P, Michelic S K, Bernhard C, Penz A and Rössler R 2019 Study on the Influence of FeTi-Addition on the Inclusion Population in Ti-Stabilized ULC Steels and Its Consequences for SEN-Clogging *Steel Res Int* **90** 1800635
[15] Deng X, Ji C, Cui Y, Tian Z, Yin X, Shao X, Yang Y and McLean A 2017 Formation and evolution of macro inclusions in IF steels during continuous casting *Ironmaking & Steelmaking* **44** 739–49
[16] Zhang L, Wang Y and Zuo X 2008 Flow Transport and Inclusion Motion in Steel Continuous-Casting Mold under Submerged Entry Nozzle Clogging Condition *Metallurgical and Materials Transactions B* **39** 534–50
[17] Hua C, Bao Y and Wang M 2021 Numerical simulation and industrial application of nozzle clogging in bilateral-port nozzle *Powder Technol* **393** 405–20
[18] Thomas B G, Yuan Q, Mahmood S, Liu R and Chaudhary R 2014 Transport and Entrapment of Particles in Steel Continuous Casting *Metallurgical and Materials Transactions B* **45** 22–35
[19] Pfeiler C, Thomas B G, Wu M, Ludwig A and Kharicha A 2008 Solidification and Particle Entrapment during Continuous Casting of Steel *Steel Res Int* **79** 599–607
[20] Yuan Q, Thomas B G and Vanka S P 2004 Study of transient flow and particle transport in continuous steel caster molds: Part II. Particle transport *Metallurgical and Materials Transactions B* **35** 703–14
[21] Ni P, Jonsson L T I, Ersson M and Jönsson P G 2014 The Use of an Enhanced Eulerian Deposition Model to Investigate Nozzle Clogging During Continuous Casting of Steel *Metallurgical and Materials Transactions B* **45** 2414–24
[22] Ni P, Jonsson L T I, Ersson M and Jönsson P G 2014 On the deposition of particles in liquid metals onto vertical ceramic walls *International Journal of Multiphase Flow* **62** 152–60
[23] Botelho T, Medeiros G, Ramos G L and Costa e Silva A 2017 The Application of Computational Thermodynamics in the Understanding and Control of Clogging and Scum in Continuous Casting of Steel *J Phase Equilibria Diffus* **38** 201–7

[24] Lee J-H and Kang Y-B 2020 Kinetics of CO Gas Dissolution into Stirred Liquid Fe at 1823 K and Its Impact on Nozzle Clogging during Continuous Casting *ISIJ International* **60** 258–66
[25] Li G, Lu C, Gan M, Wang Q and He S 2022 Influence of Submerged Entry Nozzle Clogging on the Flow Field and Slag Entrainment in the Continuous Casting Mold by the Physical Model *Metallurgical and Materials Transactions B* **53** 1436–45
[26] Barati H, Wu M, Michelic S, Ilie S, Kharicha A, Ludwig A and Kang Y-B 2021 Mathematical Modeling of the Early Stage of Clogging of the SEN During Continuous Casting of Ti-ULC Steel *Metallurgical and Materials Transactions B* **52** 4167–78
[27] Barati H, Wu M, Kharicha A and Ludwig A 2018 A transient model for nozzle clogging *Powder Technol* **329** 181–98
[28] Barati H, Wu M, Holzmann T, Kharicha A and Ludwig A 2018 Simulation of Non-metallic Inclusion Deposition and Clogging of Nozzle *CFD Modeling and Simulation in Materials Processing 2018* ed L Nastac, K Pericleous, A S Sabau, L Zhang and B G Thomas (Cham: Springer International Publishing) pp 149–58
[29] Barati H, Wu M, Kharicha A and Ludwig A 2019 Calculation Accuracy and Efficiency of a Transient Model for Submerged Entry Nozzle Clogging *Metallurgical and Materials Transactions B* **50** 1428–43
[30] Janis D, Karasev A, Inoue R and Jönsson P G 2015 A Study of Cluster Characteristics in Liquid Stainless Steel and in a Clogged Nozzle *Steel Res Int* **86** 1271–8
[31] Pilling J and Hellawell A 1996 Mechanical deformation of dendrites by fluid flow *Metallurgical and Materials Transactions A* **27** 229–32
[32] Nakamoto M, Tanaka T, Suzuki M, Taguchi K, Tsukaguchi Y and Yamamoto T 2014 Effects of Interfacial Properties between Molten Iron and Alumina on Neck Growth of Alumina Balls at Sintering in Molten Iron *ISIJ International* **54** 1195–203
[33] Uemura K, Takahashi M, Koyama S and Nitta M 1992 Filtration Mechamism of Non-metallic Inclusions in Steel by Ceramic Loop Filter. *ISIJ International* **32** 150–6
[34] Sambasivam R 2006 Clogging resistant submerged entry nozzle design through mathematical modelling *Ironmaking & Steelmaking* **33** 439–53